Article

Developmental Cell

Formation of a Snf1-Mec1-Atg1 Module on Mitochondria Governs Energy Deprivation-Induced Autophagy by Regulating Mitochondrial Respiration

Graphical Abstract

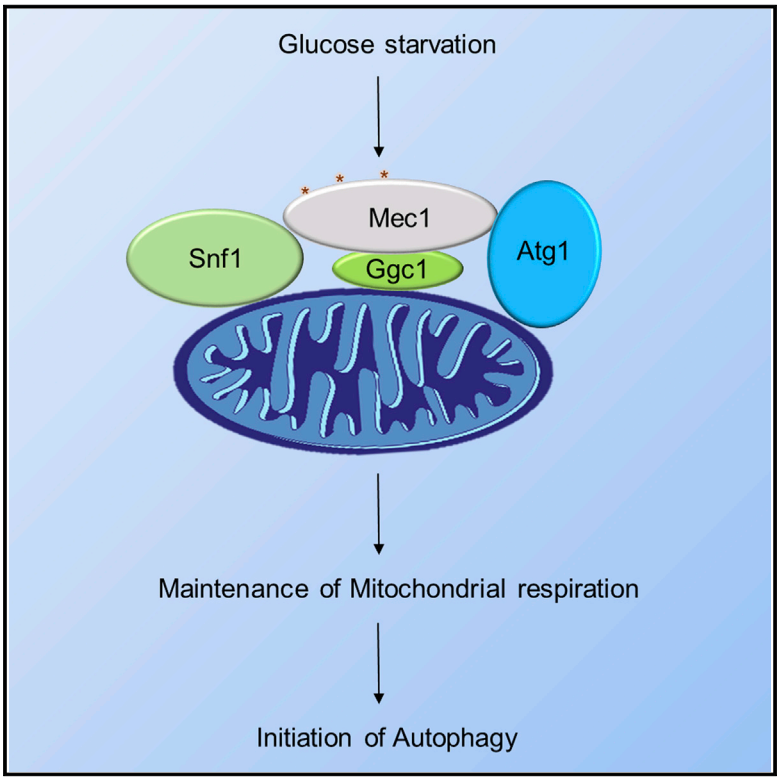

Authors

Cong Yi, Jingjing Tong, Puzhong Lu, ..., Haiteng Deng, Hongliang Li, Li Yu

Correspondence

liyulab@mail.tsinghua.edu.cn

In Brief

Yi, Tong et al. study the mechanisms underlying induction of autophagy during energy deprivation. They show that Mec1/ATR, a component of the DNA damage response pathway, is essential for glucose starvation-induced autophagy and that a Snf1-Mec1-Atg1 module on the surface of mitochondria governs energy deprivation-induced autophagy by regulating mitochondrial respiration.

Highlights

- Mec1 is essential for glucose starvation-induced autophagy
- Glucose starvation triggers the recruitment of Snf1-Mec1-Atg1-Atg13 to mitochondria
- Mitochondrial respiration is required for glucose starvation-induced autophagy
- Snf1-Mec1-Atg1 module regulates mitochondrial respiration during glucose starvation

Yi et al., 2017, Developmental Cell *41*, 59–71
April 10, 2017
http://dx.doi.org/10.1016/j.devcel.2017.03.007

Developmental Cell
Article

Formation of a Snf1-Mec1-Atg1 Module on Mitochondria Governs Energy Deprivation-Induced Autophagy by Regulating Mitochondrial Respiration

Cong Yi,[1,7] Jingjing Tong,[1,7] Puzhong Lu,[1] Yizheng Wang,[1] Jinxie Zhang,[2] Chen Sun,[4] Kangning Yuan,[1] Renyu Xue,[1] Bing Zou,[1] Nianzhong Li,[1] Shuhua Xiao,[1] Chong Dai,[1] Yuwei Huang,[1] Liling Xu,[2] Lin Li,[5] She Chen,[5] Di Miao,[3] Haiteng Deng,[3] Hongliang Li,[6] and Li Yu[1,8,*]

[1]The State Key Laboratory of Membrane Biology, Tsinghua University-Peking University Joint Centre for Life Sciences, School of Life Sciences
[2]School of Life Sciences
[3]Proteomics Facility, School of Life Science
[4]The State Key Laboratory of Membrane Biology, School of Life Science Tsinghua University, Beijing 100084, China
[5]Proteomics Centre, National Institute of Biological Sciences, Beijing 102206, China
[6]Cardiovascular Research Institute of Wuhan University, JieFang Road 238, Wuhan 430060, China
[7]Co-first author
[8]Lead Contact
*Correspondence: liyulab@mail.tsinghua.edu.cn
http://dx.doi.org/10.1016/j.devcel.2017.03.007

SUMMARY

Autophagy is essential for maintaining glucose homeostasis, but the mechanism by which energy deprivation activates autophagy is not fully understood. We show that Mec1/ATR, a member of the DNA damage response pathway, is essential for glucose starvation-induced autophagy. Mec1, Atg13, Atg1, and the energy-sensing kinase Snf1 are recruited to mitochondria shortly after glucose starvation. Mec1 is recruited through the adaptor protein Ggc1. Snf1 phosphorylates Mec1 on the mitochondrial surface, leading to recruitment of Atg1 to mitochondria. Furthermore, the Snf1-mediated Mec1 phosphorylation and mitochondrial recruitment of Atg1 are essential for maintaining mitochondrial respiration during glucose starvation, and active mitochondrial respiration is required for energy deprivation-activated autophagy. Thus, formation of a Snf1-Mec1-Atg1 module on mitochondria governs energy deprivation-induced autophagy by regulating mitochondrial respiration.

INTRODUCTION

Autophagy is primarily a catabolic response to nutrient and energy deprivation, and is conserved from yeast to mammals (Klionsky, 2010). Recently, autophagy has emerged as a key mechanism for maintaining glucose homeostasis in adult animals (Karsli-Uzunbas et al., 2014). The signaling pathway controlling nutrient deprivation-induced autophagy is well characterized (Ohsumi, 2014; Stephan et al., 2010). In yeast, for example, nitrogen starvation has been shown to trigger autophagy through a mammalian target of rapamycin (mTOR)-Atg13-Atg1 cascade (Kamada et al., 2010). However, the pathway underlying energy deprivation-induced autophagy remains relatively obscure. During energy starvation, intracellular energy status is sensed by AMP-activated protein kinase (AMPK) in mammals and Snf1 in yeast. AMPK then activates autophagy through a variety of mechanisms, including direct phosphorylation of ULK1 (homologous to Atg1) and Beclin1 (homologous to Atg6) (Kim et al., 2011, 2013) and inhibition of mTOR, an autophagy repressor (Russell et al., 2014).

Mitochondria are cellular energy metabolism centers which generate most of the cell's supply of ATP by aerobic respiration and also play important roles in other cellular processes including signaling, cell death, cellular differentiation, and autophagy (Ernster and Schatz, 1981; Wallace, 2012; Quintero et al., 2006). In mammalian cells, autophagosomes are formed at endoplasmic reticulum (ER)-mitochondrion contact sites and mitochondria have been proposed as one of the sources for autophagosome membranes (Hamasaki et al., 2013; Hailey et al., 2010). In addition, mitochondrially produced reactive oxygen species (ROS) and mitochondrial respiration play important regulatory roles in autophagy (Graef and Nunnari, 2011; Li et al., 2015).

Mec1 is a member of the phosphoinositide 3-kinase (PI3K)-related protein kinase family, which plays a central role in the DNA damage response (Kato and Ogawa, 1994; Weinert et al., 1994). Mec1 and its mammalian homolog ATR are required for cell-cycle arrest and transcriptional responses to damaged DNA. Mec1 is also involved in regulating dNTP pools and telomere length (Rodriguez and Tsukiyama, 2013; Gupta et al., 2013). ATR can modulate nuclear envelope plasticity and chromatin association with the nuclear envelope when the cell faces mechanical forces (Kumar et al., 2014). Recently, ATM, another member of the PI3K-related protein kinase family, which is also important for the response to DNA damage, was shown to play an essential role in regulating pexophagy in response to ROS

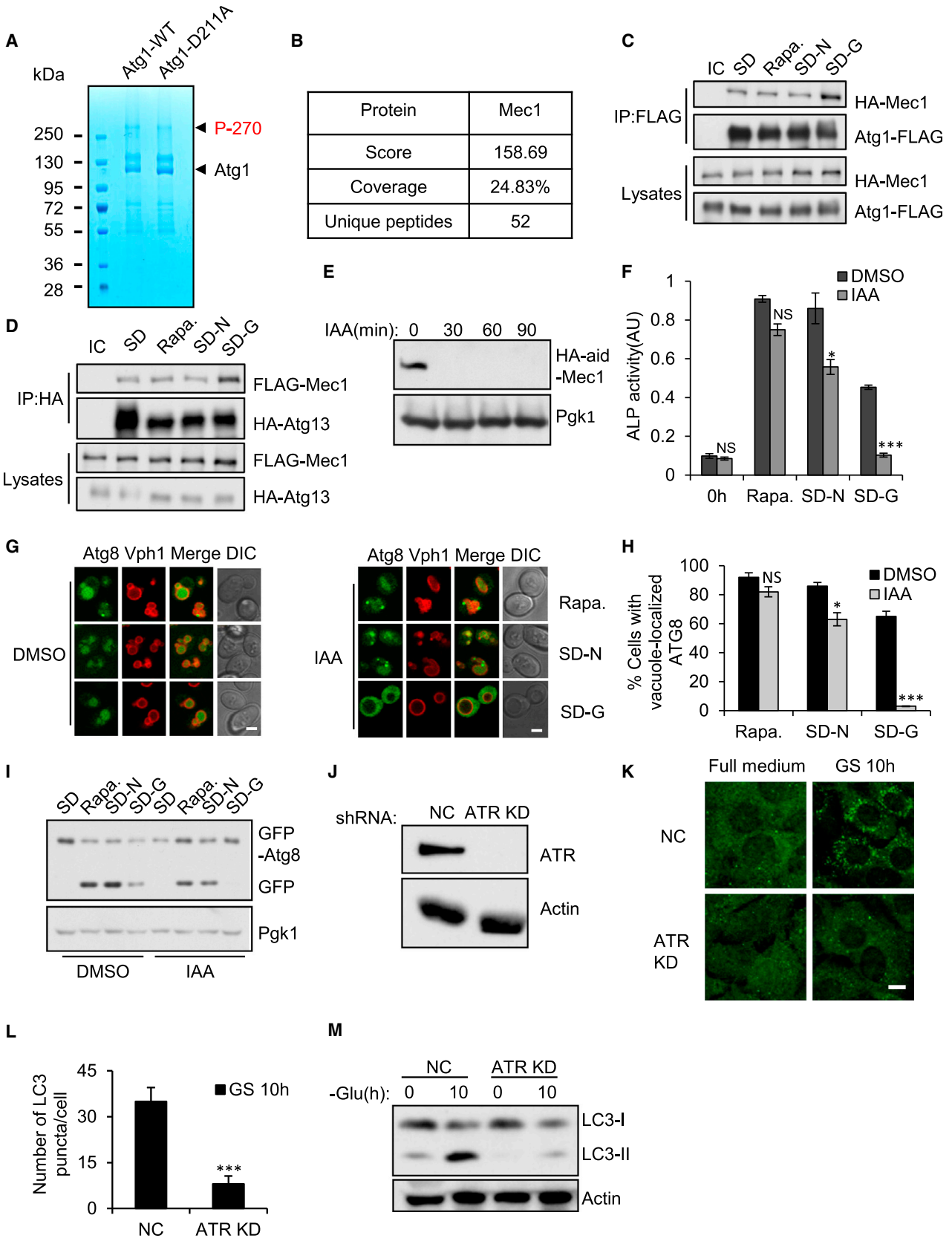

(legend on next page)

(Zhang et al., 2015). Here we describe a role of a Snf1-Mec1-Atg1 module in the initiation of autophagy in response to energy deprivation.

RESULTS

Mec1 Is Essential for Glucose Starvation-Induced Autophagy

Our effort to purify Atg1 from yeast under nitrogen starvation conditions revealed that both Atg1 and $Atg1^{D211A}$, a mutant that lacks kinase activity (Matsuura et al., 1997), stably bind to a protein with a molecular weight of around 270 kDa (Figure 1A). Mass spectrometry identified this protein as Mec1 (Figure 1B). Interestingly, glucose starvation, but not other autophagy stimuli, markedly enhances the interaction between Atg1 and Mec1 (Figure 1C). Similarly, glucose starvation also enhances the interaction between Mec1 and Atg13 (Figure 1D).

Since Mec1 is essential for yeast growth, we tested the role of Mec1 in autophagy by conditionally knocking down Mec1 expression using the auxin-inducible degron (AID) system (Nishimura et al., 2009). As shown in Figure 1E, treating cells with IAA causes rapid degradation of Mec1. Knock down of Mec1 completely blocks glucose starvation-induced autophagy, but only slightly impairs autophagy induced by nitrogen starvation (Figures 1F–1I) (Noda et al., 1995; Kirisako et al., 1999). To test whether the role of Mec1 in autophagy is evolutionarily conserved, we stably knocked down ATR (homologous to Mec1) in normal rat kidney cells, and found that glucose starvation-induced autophagy was markedly decreased (Figures 1J–1M). This indicates that ATR is important for glucose starvation-induced autophagy in mammals.

Using the same approach, we deleted or conditionally depleted other members of the DNA repair pathway, including Tel1, Lcd1, Ddc1, and Rad53 (Jackson, 1996; Majka et al., 2006), and found that absence or reduced levels of these proteins does not affect glucose starvation-induced autophagy (Figure S1). Thus, Mec1, but not the whole DNA repair pathway, participates in regulation of glucose starvation-induced autophagy.

Glucose Starvation Triggers Translocation of Snf1, Mec1, Atg1, and Atg13 to Mitochondria

Under energy-rich conditions, Mec1 has a diffuse localization pattern, while glucose starvation, but not other autophagic stimuli, induces formation of Mec1 foci (Figure 2A). Mec1 foci are transiently induced; the number of cells with Mec1 foci and the number of Mec1 foci per cell peaked at 1 hr after glucose starvation, and almost no Mec1 foci were visible 4 hr after glucose starvation. Adding glucose back quickly reduced the number of Mec1 foci (Figures 2C, 2D, S2A, and S2B). Co-localization analysis shows that the majority of Mec1 foci co-localize with the mitochondrial marker Om45 (Figures 2B and 2E), but not with the peroxisome marker Pex14 (Figure S2C and 2D).

To verify the recruitment of Mec1 to mitochondria, we purified mitochondria from cells growing in nutrient-rich conditions or undergoing glucose starvation. The mitochondrial fractions were tested for possible contamination with cytoplasm and organelles including ER, endosome, nuclei, and vacuoles. We did not detect marker proteins from these organelles in the purified mitochondrial fractions (Figure 2F). There is no detectable Mec1 on mitochondria from yeast grown in nutrient-rich conditions; however, 1 hr of glucose starvation triggers translocation of Mec1 to mitochondria (Figure 2F). Similarly, glucose starvation induces translocation of Snf1 to mitochondria (Figure 2F). Treating purified mitochondria with protease K completely degrades Snf1, Mec1, and the outer mitochondrial membrane marker Tom70, but not the inner mitochondrial member marker Tim23 (Figure 2F) (Hines et al., 1990; Emtage and Jensen, 1993). This indicates that

Figure 1. Mec1 Regulates Glucose Starvation-Induced Autophagy

(A) Atg1 wild-type (WT) and Atg1 D211A (atg1-KD) proteins were purified from FLAG-tagged Atg1 WT- or Atg1 D211A-expressing cells after nitrogen starvation for 1 hr. The purified proteins were separated by 4%–15% SDS-PAGE and subjected to liquid chromatography-tandem mass spectrometry (LC-MS/MS) analysis.

(B) Identification of Mec1 by LC-MS/MS analysis.

(C) Cells expressing HA-Mec1 and Atg1-FLAG were cultured in nitrogen starvation medium (SD-N), glucose starvation medium (SD-G), or treated with rapamycin (0.2 μg/mL) for 1 hr. Cell lysates were immunoprecipitated with anti-FLAG antibody and analyzed by western blot using anti-HA antibody. IC, mouse IgG1 isotype control.

(D) Cells expressing FLAG-Mec1 and HA-Atg13 were treated as in (C). Cell lysates were immunoprecipitated with anti-HA antibody and analyzed using the indicated antibodies. IC, mouse IgG1 isotype control.

(E) Cells expressing 3XHA-Aid-Mec1 with the endogenous promoter were treated with 0.5 mM IAA for the indicated times. The Mec1 levels were monitored by western blot.

(F) *pho13*Δ and *pho8*Δ*60* Cells expressing 3XHA-Aid-Mec1 with the endogenous promoter were treated with DMSO or IAA for 2 hr, and then subjected to SD-N, SD-G, or rapamycin treatment in the presence or absence of IAA for 4 hr. Autophagy activity was assessed by ALP assay. n = 3 independent experiments were quantified. Data are presented as means ± SD. ***$p < 0.001$, *$p < 0.05$; NS, not significant; two-tailed Student's t tests were used.

(G) Cells expressing 3XHA-Aid-Mec1, GFP-Atg8, and Vph1-Cherry were treated as in (F). Autophagy activity was assessed by translocation of GFP-Atg8 into vacuoles. Scale bar, 2 μm.

(H) Cells from (G) were analyzed for translocation of GFP-Atg8 into vacuoles. n = 300 cells pooled from three independent experiments. Data are presented as means ± SD. ***$p < 0.001$, *$p < 0.05$; NS, not significant; two-tailed Student's t tests were used.

(I) Cells from (G) were analyzed by western blot for GFP-Atg8 cleavage.

(J) ATR expression levels in NC (non-specific control) and ATR stable knockdown NRK (normal rat kidney) cells were analyzed by western blot with ATR antibody.

(K) NC or ATR knockdown cells were starved in glucose-free medium (GS) for 10 hr and stained by LC3 antibody. Scale bar, 10 μm.

(L) Cells from (K) were quantified for the number of autophagosomes in a blind fashion. Fifty cells were counted. n = 3 independent experiments were quantified. Data are presented as means ± SD. ***$p < 0.001$; two-tailed Student's t tests were used.

(M) NC or ATR knockdown cells were starved in glucose-free medium for 10 hr. The autophagy activity in cell samples was assessed by western blot for LC3 processing.

See also Figure S1.

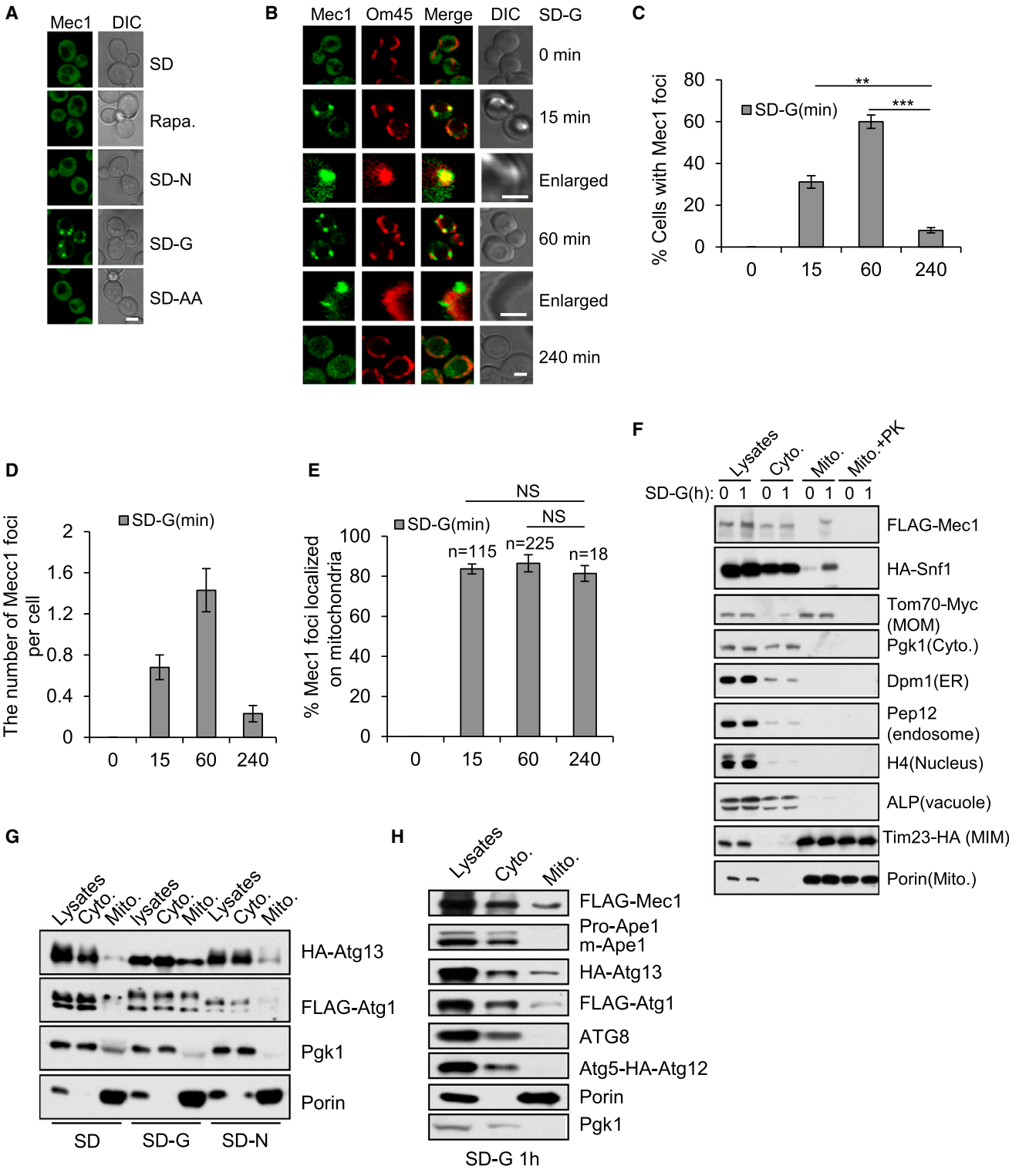

Figure 2. Recruitment of Snf1, Mec1, Atg1, and Atg13 to Mitochondria under Glucose Starvation Conditions

(A) Cells expressing GFP-Mec1 were cultured in SD-N, SD-G, or amino acid starvation medium (SD-AA), or with rapamycin for 1 hr, then analyzed by microscopy. Scale bar, 2 μm.

(B) Images of cells expressing GFP-Mec1 and Om45-Cherry which were cultured in SD-G for the indicated times. Scale bar, 2 μm.

(C and D) Cells from (B) in SD-G were quantified for the number of cells with Mec1 foci and the number of Mec1 foci per cell. n = 300 cells pooled from three independent experiments. Data are presented as means ± SD. ***$p < 0.001$, **$p < 0.01$ by two-tailed Student's t tests.

(legend continued on next page)

Snf1 and Mec1 are located on the outer surface of mitochondria. These data indicate that glucose starvation causes recruitment of Snf1 and Mec1 to mitochondria. It is worth noting that all the results are consistent with mitochondrial localization, but we cannot rule out a possibility that the proteins are instead localizing to another structure close to or associated with the mitochondria.

The fact that Mec1 binds to Atg1 and Atg13, and that Mec1 foci are largely recruited to mitochondria, prompted us to test the localization of Atg1 and Atg13 after different autophagic stimuli. Biochemical analysis of purified mitochondria confirmed the recruitment of Atg1 and Atg13 to mitochondria after glucose starvation (Figure 2G); in contrast, the pre-autophagosomal structure (PAS) marker Ape1 or the isolation membrane markers Atg5-12 and Atg8 are not translocated to mitochondria after glucose starvation (Figure 2H) (Yen et al., 2007; Mizushima, 2009). Taken together, these data indicate that glucose starvation causes recruitment of Snf1, Mec1, Atg1, and Atg13, but not PAS/isolation membrane markers, to mitochondria.

Snf1-Mediated Mec1 Phosphorylation Is Essential for Glucose Starvation-Induced Autophagy

In yeast, the intracellular energy status is sensed by Snf1, the homolog of AMPK (Mitchelhill et al., 1994). Snf1 is essential for glucose starvation-induced autophagy (Figure S3A and S3B), and glucose starvation triggers the translocation of Snf1 to mitochondria (Figure 2F). We therefore studied the possible link between Snf1 and Mec1. First, we checked whether Mec1 can be phosphorylated by Snf1. The similarity between AMPK and Snf1 prompted us to test whether the commercially available phospho-(Ser/Thr) AMPK substrate (P-S/T2-102) antibody, which recognizes the LXRXXpS/pT motif (Gwinn et al., 2008), can also recognize Snf1-mediated phosphorylation. We found that glucose starvation, but not nitrogen starvation or rapamycin treatment, can induce phosphorylation of LXRXXpS/pT in Mec1 (Figures 3A and S3C). Glucose starvation-induced Mec1 phosphorylation is abolished in *SNF1* null cells or cells expressing a Snf1 mutant which lacks kinase activity ($snf1^{T210A}$, hereafter referred to as $snf1^{kd}$; McCartney and Schmidt, 2001; Figure 3B). This confirms that Mec1 phosphorylation recognized by the phospho-(Ser/Thr) AMPK substrate (P-S/T2-102) antibody is indeed mediated by Snf1. Mec1 contains three LXRXXpS/pT motifs, ending at positions S552, T797, and T1074 (Figure 3C). To determine which of these sites is phosphorylated, we mutated them individually or in various combinations, and then tested the phosphorylation level of the mutant proteins upon glucose starvation. We found that glucose starvation-induced phosphorylation of Mec1 is abolished in the $mec1^{S552A\text{-}T797A\text{-}T1074A}$ mutant strain (hereafter referred to as $mec1^{3A}$, Figure 3D), and the $Mec1^{3A}$ mutant protein cannot be phosphorylated by Snf1 in vitro (Figure 3E). Thus, we conclude that Snf1 phosphorylates Mec1 at S552, T797, and T1074.

Next, to test whether phosphorylation of Mec1 by Snf1 is required for autophagy, we cultured wild-type and mutant strains in growth medium and then divided each batch of yeast into nitrogen starvation medium (SD-N) and glucose starvation medium (SD-G) (Figure 3F). We found that glucose starvation failed to induce autophagy in the $mec1^{3A}$ and $mec1^{T797A}$ mutant strains (Figures 3G, 3H, and S3D). Further analysis showed that mitochondrial recruitment of Mec1 is markedly increased in mec1-3A cells (Figure 3I). In contrast, the recruitment of Atg1 to mitochondria is impaired in mec1-3A, *SNF1* null, and IAA-treated Mec1-AID cells, indicating that the recruitment of Atg1 to mitochondria is dependent on Snf1-mediated Mec1 phosphorylation (Figures 3J–3L). Moreover, we found that $Mec1^{3A}$ can still bind Atg13 upon glucose starvation (Figure 3M), while the interaction between Atg1 and $Mec1^{3A}$ is impaired (Figure 3N). This implies that Atg1 is recruited to mitochondria by phosphorylated Mec1.

Ggc1 Is Required for the Recruitment of Mec1 to Mitochondria and for Glucose Starvation-Induced Autophagy

We hypothesized that recruitment of Mec1 to mitochondria is required for glucose starvation-induced autophagy. We therefore decided to identify the adaptor protein which is required for mitochondrial localization of Mec1. We took advantage of the fact that Mec1 accumulates on mitochondria in $snf1^{kd}$ cells (Figure S3E). First, we purified mitochondria from starved $snf1^{kd}$ cells or FLAG-Mec1-expressing $snf1^{kd}$ cells. Mitochondrion-associated proteins were extracted using a lysis buffer containing 1% SDS. The SDS concentration in the lysis buffer was then diluted to 0.1% and Mec1, and its associated proteins were immunoprecipitated with an anti-FLAG antibody and analyzed by mass spectrometry (Figure S3F) (Wang et al., 2012).

By this approach, we identified Ggc1, a mitochondrial protein containing six transmembrane domains (Vozza et al., 2004), as a potential Mec1-binding protein (Figures 4A and 4B). We found that Ggc1 localized on both the outer and inner mitochondrial membranes (Figure 4C). The interaction between Mec1 and Ggc1 was verified by immunoprecipitation (Figure 4D). Next, we generated *GGC1* null cells (*ggc1*Δ) and found that glucose starvation-induced recruitment of Mec1 to mitochondria is impaired in these cells (Figure 4E). Thus, Mec1 is recruited to mitochondria via Ggc1. In *ggc1*Δ cells, glucose starvation-induced autophagy is completely blocked (Figures 4F–4H), indicating that mitochondrial recruitment of Mec1 is required for glucose starvation-induced autophagy. Furthermore, we found that the kinase activity of Snf1 was not decreased in *ggc1*Δ cells (Figure 4I), while Snf1-mediated Mec1 phosphorylation is

(E) Cells from (B) were quantified for mitochondrial GFP-Mec1 foci at all time-points. n, the number of Mec1 foci that were analyzed in 300 cells pooled from three independent experiments. Data are presented as means ± SD. NS, not significant by two-tailed Student's t tests. Scale bar, 2 μm.

(F) Cells expressing FLAG-Mec1, HA-Snf1, Tom70-Myc, and Tim23-HA were cultured in SD or SD-G for 1 hr and harvested. Mitochondria were purified and treated with protease K (PK) or not. Samples were analyzed by western blot using the indicated antibodies.

(G) Cells expressing FLAG-Atg1 and HA-Atg13 were starved in SD-N or SD-G, or cultured in full medium (SD). Mitochondria were extracted and different fractions were analyzed by western blots with the indicated antibodies.

(H) Cells expressing FLAG-Mec1, HA-Atg13, FLAG-Atg1, and Atg5-HA-Atg12 were cultured in SD-G for 1 hr. Mitochondria were purified and different fractions were analyzed by western blots with the indicated antibodies. See also Figure S2.

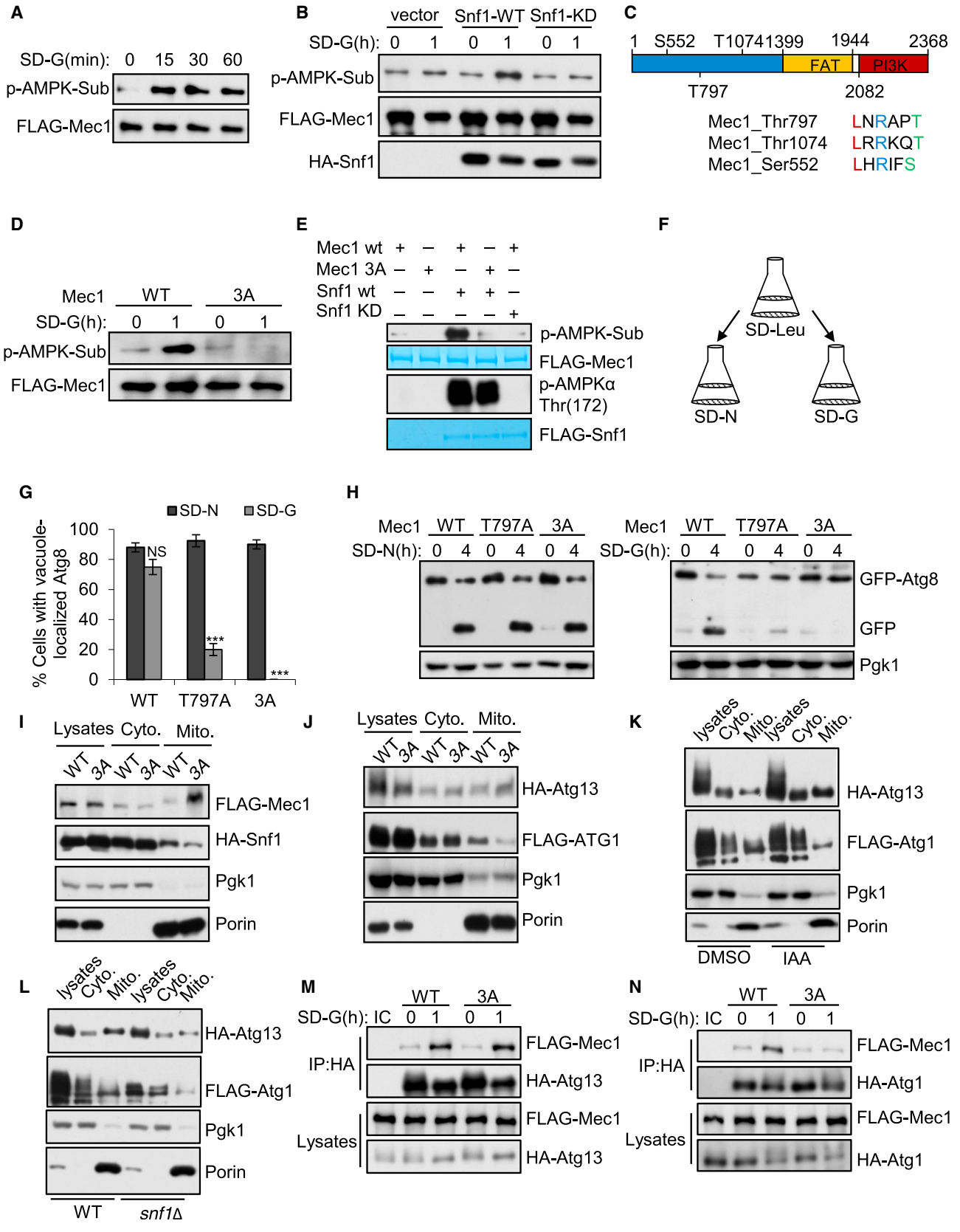

(legend on next page)

not induced (Figure 4J). These results indicate that Mec1 phosphorylation occurs on mitochondria, and recruitment of Mec1 to mitochondria via Ggc1 is required for phosphorylation of Mec1.

Mitochondrial Respiration Is Essential for Glucose Starvation-Induced Autophagy

Next, we studied the role of mitochondria in glucose starvation-induced autophagy. We serendipitously discovered that glucose starvation-induced autophagy, but not autophagy induced by nitrogen starvation or rapamycin treatment, was markedly impaired when cells are grown in sealed tubes (Figures 5A and 5B). This observation prompted us to test whether aerobic respiration is also required for glucose starvation-induced autophagy. We generated mutants in which genes encoding components of the electron transport chain or pyruvate dehydrogenase complex were deleted. We also tested the *PET100* null mutant, which is well established as a respiration-defective strain (Church et al., 1996). In all mutants except *nde1*Δ, the oxygen consumption is dramatically reduced under glucose starvation conditions (Figure 5C), indicating that aerobic respiration is defective in these mutants. Interestingly, we found that all mutants with defective aerobic respiration also have defective glucose starvation-induced autophagy; in contrast, nitrogen starvation-induced autophagy is not affected in these mutants (Figures 5D and 5E). We also analyzed the recruitment of Mec1 to mitochondria in respiration-deficient cells and autophagy-deficient cells. We found that mitochondrially localized Mec1 foci accumulated in both types of cell (Figure S4), indicating that respiration is not required for mitochondrial recruitment of Mec1. Since Ggc1 has been shown to be essential for mitochondrial genome maintenance and for respiration (Vozza et al., 2004), these data imply that the role of Ggc1 in recruitment of Mec1 is independent from its role in regulation of mitochondrial respiration.

A Snf1-Mec1-Atg1 Module Is Essential for Maintaining Mitochondrial Respiration during Glucose Starvation

The fact that mitochondrial respiration is essential for glucose starvation-induced autophagy prompted us to probe the potential link between the mitochondrially localized Snf1-Mec1-Atg1 module and mitochondrial respiration. We found that, under glucose starvation conditions, mitochondrial respiration is almost completely lost in *SNF1* null, Snf1-KD, IAA-treated Mec1-AID, Mec1-3A, ATG1 null, and Atg1-KD cells, while in nutrient-rich and nitrogen starvation conditions, mitochondrial respiration is comparable between wild-type and mutant cells. These data indicate that the Snf1-Mec1-Atg1 cascade is essential for maintaining mitochondrial respiration during glucose starvation (Figures 6A–6D).

The participation of Atg1 in regulation of mitochondrial respiration prompted us to test whether other ATG genes, especially Atg13, are required for maintaining mitochondrial respiration during autophagy. For this purpose, we tested the mitochondrial respiration in Atg1, Atg3, Atg4, Atg5, Atg9, Atg10, Atg13, Atg14, and Atg17 null cells. As shown in Figure 6E, we found that Atg1 is the only ATG gene that affects mitochondrial respiration. Thus, Atg1, rather than autophagy as a cellular process, is required for maintaining mitochondrial respiration under glucose starvation conditions.

Next, we studied how mitochondrial respiration affects autophagy. We found that, in respiration-defective cells, the activation of Snf1 is not impaired and Mec1 accumulates (Figure S5A and S5B). However, Snf1-mediated Mec1 phosphorylation is not induced in mitochondrial mutants (Figure S5C and S5D). Moreover, the interaction between Atg1 and Atg13 is impaired in *NDI1* and *COX6* null cells (Figure S6A). Similarity, the interaction between Atg1 and Atg13 is impaired in IAA-treated Mec1-AID, Mec1-3A, and *ggc1*Δ cells under glucose starvation conditions, indicating that the Atg1/Atg13 interaction is dependent on mitochondrial respiration (Figures S6B–6D). Surprisingly, we

Figure 3. Snf1-Mediated Mec1 Phosphorylation Is Essential for Glucose Starvation-Induced Autophagy

(A) FLAG-Mec1-expressing cells underwent glucose starvation for the indicated time. Phosphorylation of immunoprecipitated FLAG-Mec1 was tested by immunoblotting with phospho-(Ser/Thr) AMPK substrate antibody.

(B) pRS316, HA-Snf1 WT, or HA-Snf1-KD were expressed in FLAG-Mec1-expressing *snf1*Δ cells, which underwent SD-G for 0 or 1 hr. Phosphorylation of immunoprecipitated FLAG-Mec1 was tested as in (A).

(C) The Snf1 consensus phosphorylation motifs in the Mec1 protein.

(D) Cell lysates were prepared from 3XFLAG-Mec1- and 3XFLAG-Mec1$^{S552A-T797A-T1074A}$ (Mec1^{3A})-expressing cells grown in SD-G for 0 or 1 hr. Phosphorylation of immunoprecipitated FLAG-tagged Mec1 was tested as in (A).

(E) In vitro phosphorylation of Mec1 by Snf1. WT or mutant Mec1 protein was purified from *snf1*Δ cells expressing 3XFLAG-Mec1 and 3XFLAG-Mec1-3A. WT or mutant Snf1 protein was purified from glucose-starved *snf1*Δ cells expressing 3XFLAG-Snf1 or 3XFLAG-Snf1-KD. Phosphorylation of Mec1 was tested as in (A). Snf1 kinase activity was monitored by immunoblotting with anti-phospho-AMPKα (Thr172) antibody.

(F) Diagram showing the experimental procedure for (G). Batches of cells were cultured in normal growth medium, and cells were then split and subjected to glucose or nitrogen starvation.

(G) Cells expressing GFP-Atg8 and Vph1-Cherry in WT, *mec1*$^{S552A-T797A-T1074A}$ (3A) or *mec1*^{T797A} (T797A) strains were starved in SD-N or SD-G for 4 hr. Cells were analyzed for translocation of GFP-Atg8 into vacuoles. n = 300 cells pooled from three independent experiments. Data are presented as means ± SD. ***$p < 0.001$; NS, not significant; two-tailed Student's t tests were used.

(H) Cells expressing GFP-Atg8 in WT, *mec1*$^{S552A-T797A-T1074A}$ (3A), or *mec1*^{T797A} (T797A) strains were starved in SD-N or SD-G for 4 hr. Autophagy activity was assessed by western blot analysis of GFP-Atg8 cleavage.

(I) Cells expressing FLAG-Mec1 and HA-Snf1 were cultured in SD-G for 1 hr. Mitochondria were purified and different fractions were analyzed by western blots with the indicated antibodies.

(J–L) 3XFLAG-Atg1 and HA-Atg13 were co-expressed in WT, Mec1-3A, snf1Δ, and Mec1-auxin degron strains, and the cells were subject to glucose starvation for 1 hr. Mitochondria were purified and different fractions were analyzed by western blot using the indicated antibodies.

(M and N) Association of Mec1 with Atg13 or Atg1 in WT or *mec1*^{3A} (3A) cells. Cells expressing FLAG-Mec1 and HA-Atg13, FLAG-Mec1, and HA-Atg1 were starved in SD-G for 0 and 1 hr, and cell lysates were immunoprecipitated with HA antibody and analyzed by western blot using the indicated antibodies. IC, mouse IgG1 isotype control. See also Figure S3.

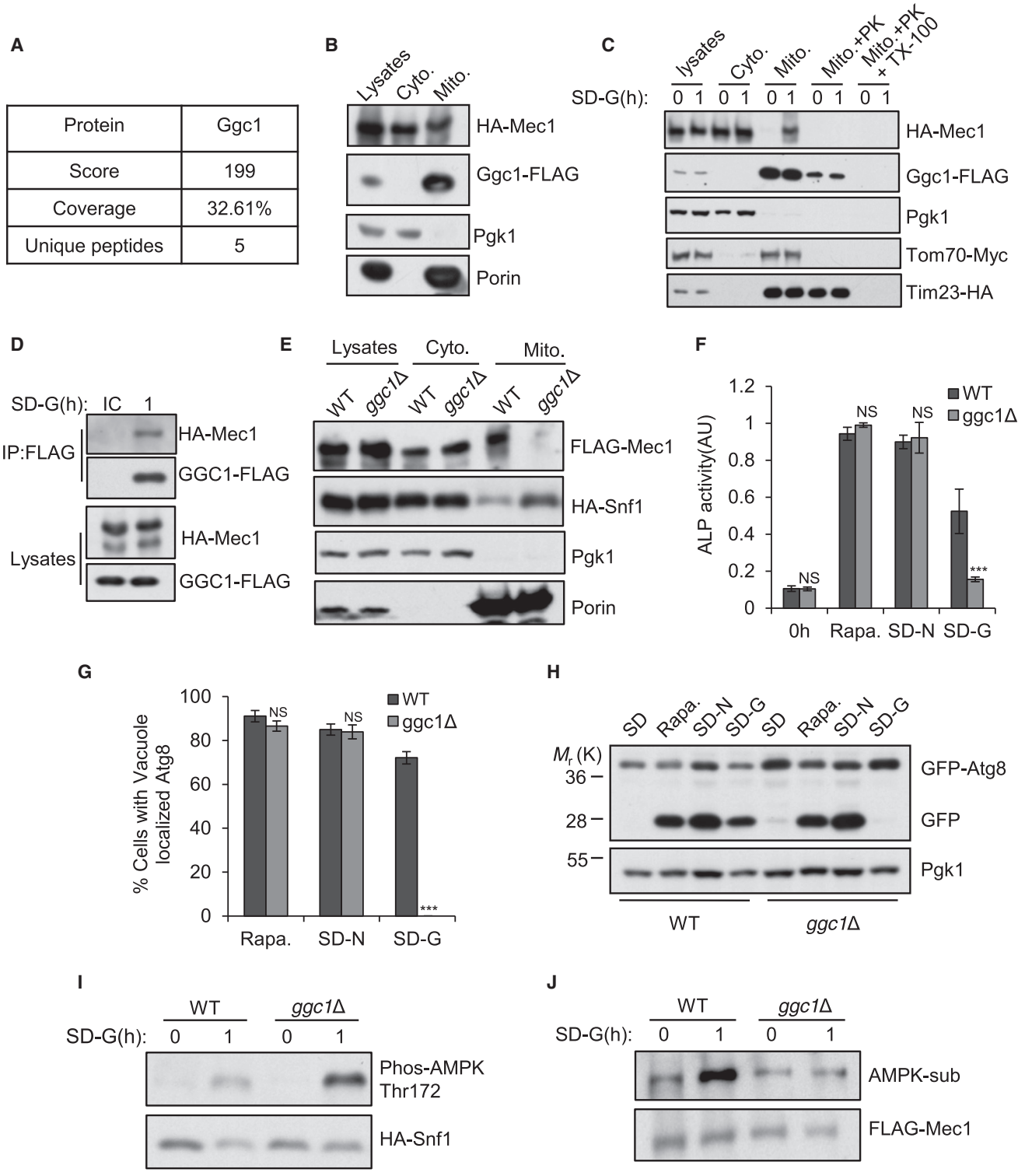

Figure 4. Ggc1 Is Required for the Recruitment of Mec1 to Mitochondria and Is Essential for Glucose Starvation-Induced Autophagy

(A) Identification of Ggc1 by LC-MS/MS. Mitochondria were purified from *snf1*^{kd} cells expressing FLAG-Mec1, and Mec1-interacting proteins were immunoprecipitated with an anti-FLAG antibody, separated by SDS-PAGE, and analyzed by LC-MS/MS. The number of unique peptides identified, the score, and the coverage of Ggc1 are listed.

(B) WT cells expressing HA-Mec1 and Ggc1-FLAG were cultured in SD-G for 1 hr, then fractionated. Mitochondrial and cytosolic fractions were analyzed by western blot with the indicated antibodies to detect the association of Mec1 with Ggc1.

(legend continued on next page)

found that, although Atg13 is required for glucose starvation-induced autophagy, the glucose starvation-induced elevation of Atg1 kinase activity is not dependent on Atg13, nor is it dependent on Mec1 or Ggc1 (Figure S7). From these data, we conclude that mitochondrial respiration is required for glucose starvation-induced Mec1 phosphorylation and Atg1/Atg13 interaction.

DISCUSSION

In summary, we found that mitochondrion-localized Mec1 regulates energy deprivation-induced autophagy. Furthermore, we identified that Snf1-mediated phosphorylation of Mec1 on the mitochondrial surface leads to recruitment of Atg1 to mitochondria, and the formation of this Snf1-Mec1-Atg1 cascade on the mitochondrial surface is essential to maintain mitochondrial respiration during glucose starvation (Figure 7). This process involves the DNA damage-sensing kinase Mec1, the energy sensor Snf1, and the autophagy protein Atg1 to regulate the activity of the cell's energy metabolism centers (mitochondria).

In this study, we demonstrated that formation of a Snf1-Mec1-Atg1 module on mitochondria is required for maintaining mitochondrial respiration during glucose starvation. At this point, we still do not know exactly how the Snf1-Mec1-Atg1 module regulates mitochondrial respiration. However, given the fact that Atg1 is localized on mitochondria and Atg1 kinase activity is required for maintaining respiration, it is reasonable to speculate that Atg1 may maintain mitochondrial respiration by directly or indirectly phosphorylating key mitochondrial proteins which are essential for respiration.

How does mitochondrial respiration regulate autophagy? Although we do not have definitive evidence, we speculate that respiration regulates autophagy by controlling the interaction between Atg1 and Atg13. In autophagy induced by other stimuli such as rapamycin treatment or nitrogen starvation, the Atg1/Atg13 interaction is essential for autophagy induction (Yamamoto et al., 2016). Atg13 carries out its function through two mechanisms: (1) binding of Atg13 can enhance the kinase activity of Atg1; (2) Atg13 is required for multimeric assembly of a supramolecular Atg1 complex, which is composed of Atg1, Atg13, and Atg17-Atg29-Atg31, by interacting with two distinct Atg17 molecules. In glucose starvation-induced autophagy, although Atg13 is not required for regulating Atg1 kinase activity, the interaction between Atg1 and Atg13 may be required for formation of the supramolecular Atg1 complex, and thus for autophagy.

On the one hand, Snf1-mediated Mec1 phosphorylation is required to maintain mitochondrial respiration; on the other hand, mitochondrial respiration is required for Snf1-mediated Mec1 phosphorylation. The reciprocal nature of Mec1 phosphorylation and mitochondrial respiration highlights the importance of this regulatory module, as impairment of either Mec1 phosphorylation or impairment of respiration can be amplified through this reciprocal loop, causing failure of autophagy induction. This module thus provides a built-in quality control mechanism for autophagy initiation which will limit autophagy induction in cells in which both mitochondrial respiration and the energy-sensing capacity are intact.

Mitochondrial respiration has been shown to be required for amino acid starvation-induced autophagy (Graef and Nunnari, 2011). In their study, Graef and Nunnari established an elegant protocol to investigate the role of mitochondria in autophagy. First, cells were grown in galactose as opposed to glucose as the carbon source. Subsequently, autophagy was induced by amino acid starvation. Various carbon sources were used during the amino acid starvation to determine its effect on autophagy. They found that when cells are starved of both carbon and amino acids, autophagy is almost completely blocked in respiration-defective Rho^0 cells. However, when various carbon sources are added during amino acid starvation, autophagy is only partially inhibited in Rho^0 cells. These results imply that carbon starvation is at least partially responsible for the dependence of amino acid/carbon starvation-induced autophagy on mitochondrial respiration.

In this study, we identified ten genes required for energy deprivation-induced autophagy but not for autophagy induced by canonical stimuli; we demonstrated that the assembly of a Snf1-Mec1-Atg1 module on the mitochondrial surface is required for energy deprivation-induced autophagy; and we also showed that the energy deprivation-induced autophagy is dependent on mitochondrial respiration. Given the large number of genes involved in maintaining mitochondrial respiration, it is likely that additional genes are also required for energy deprivation-induced autophagy. These observations imply that energy

(C) Cells expressing HA-Mec1, Ggc1-FLAG, Tim23-HA, and Tom70-Myc were cultured in full medium or SD-G for 1 hr, then harvested, and fractioned. Mitochondria were purified by sucrose gradient centrifugation then treated with protein kinase (PK) and/or Triton X-100 (TX-100). Samples were analyzed by western blot using the indicated antibodies.

(D) Association of Mec1 with Ggc1 in WT cells. Cells expressing HA-Mec1 and Ggc1-FLAG were treated as in (B). Mitochondria were lysed and immunoprecipitated with FLAG antibody and analyzed by western blot using the indicated antibodies. IC, mouse IgG1 isotype control.

(E) Ggc1 is required for recruitment of Mec1 to mitochondria. WT or *ggc1*Δ strains expressing FLAG-Mec1 and HA-Snf1 were cultured in SD-G for 1 hr. Mitochondria were purified and different fractions were analyzed by western blot using the indicated antibodies.

(F) WT and *ggc1*Δ cells with *pho13*Δ and *pho8*Δ60 were grown to OD_{600} = 0.8–1.0 and then subjected SD-N, SD-G, or rapamycin treatment for 4 hr. Autophagy activity was assessed by ALP assay. n = 3 independent experiments were quantified. Data are presented as means ± SD. ***p < 0.001; NS, not significant; two-tailed Student's t tests were used.

(G) Cells expressing GFP-Atg8 and Vph1-Cherry in WT or *ggc1*Δ strains were starved in SD-N or SD-G, or treated with rapamycin for 4 hr. Autophagy activity was assessed by translocation of GFP-Atg8 into vacuoles. n = 300 cells pooled from three independent experiments. Data are presented as means ± SD. ***p < 0.001; NS, not significant; two-tailed Student's t tests were used.

(H) Cells from (G) were analyzed for autophagy activity by western blot analysis of GFP-Atg8 cleavage.

(I) WT and *ggc1*Δ cells expressing HA-Snf1 were grown in SD-G for 0 or 1 hr. Cell lysates were prepared and samples were tested by immunoblotting with phospho-AMPK Thr172 antibody.

(J) Cell lysates were prepared from FLAG-Mec1-expressing WT and *ggc1*Δ cells that were grown in SD-G for 0 or 1 hr. Phosphorylation of immunoprecipitated FLAG-tagged Mec1 was tested by immunoblotting with phosphor-(Ser/Thr) AMPK substrate antibody. See also Figure S4.

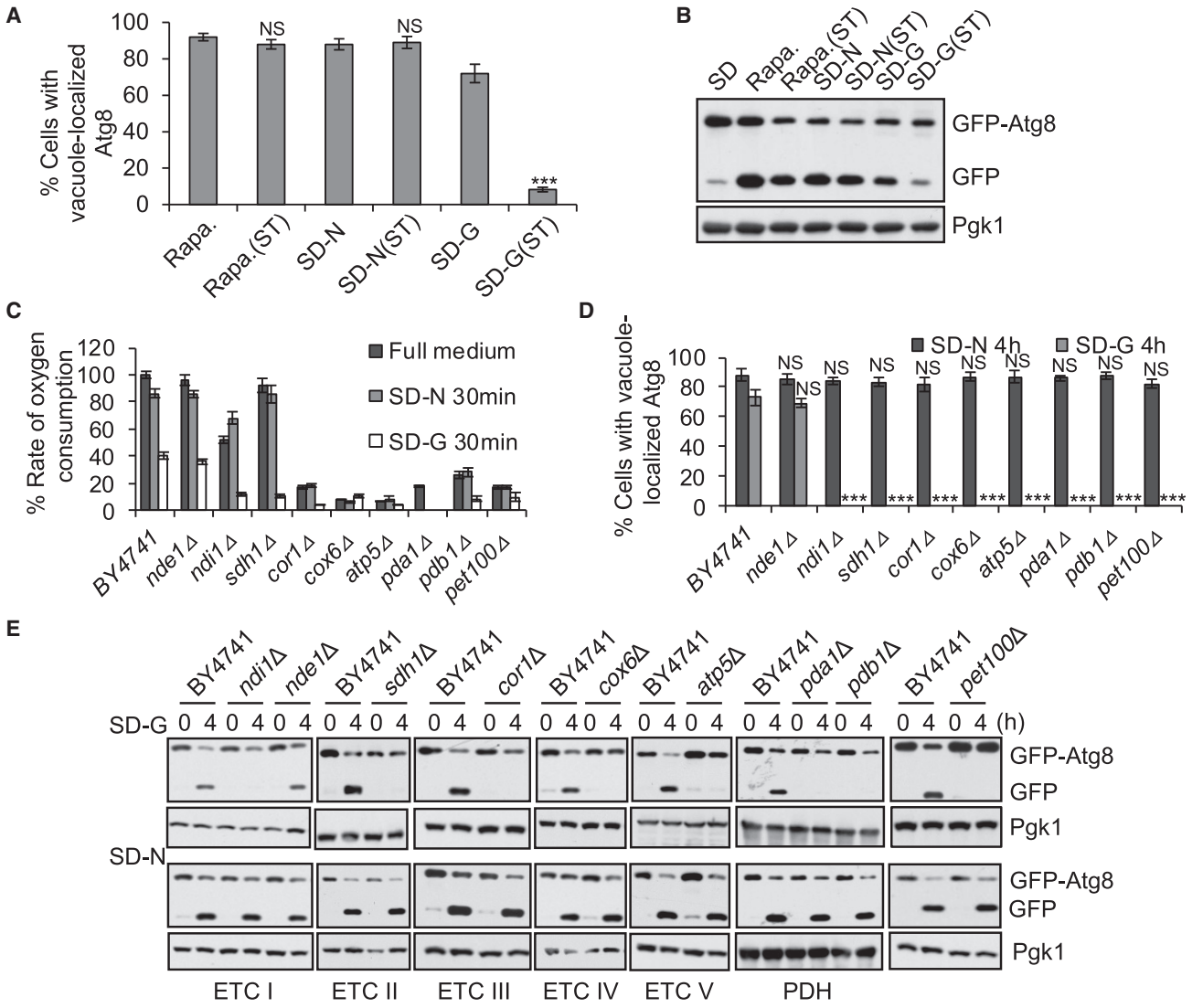

Figure 5. Mitochondrial Respiration Is Required for Glucose Starvation-Induced Autophagy

(A) WT (BY4741) cells expressing GFP-Atg8 and Vph1-Cherry were cultured in normal growth medium, then split, and subjected to glucose starvation, nitrogen starvation, or rapamycin treatment in regular tubes or sealed tubes (ST) for 4 hr. Autophagy activity was assessed by translocation of GFP-Atg8 into vacuoles, as judged by confocal microscopy. n = 300 cells pooled from three independent experiments. Data are presented as means ± SD. ***$p < 0.001$; NS, not significant; two-tailed Student's t tests were used.

(B) Autophagy activity was assessed in cells from (A) by western blot analysis of GFP-Atg8 cleavage.

(C) WT (BY4741), *nde1*Δ, *ndi1*Δ, *sdh1*Δ, *cor1*Δ, *cox6*Δ, *atp5*Δ, *pda1*Δ, *pdb1*Δ, and *pet100*Δ strains were cultured in SD-G or SD-N for 30 min. Cells were harvested and oxygen consumption was measured using a Clark-type oxygen electrode from a single experiment, n = 3 independent experiments were quantified. Data are presented as means ± SD.

(D) GFP-Atg8 was expressed in the strains from (C). Cells were grown to log-growth phase, then split, and subjected to glucose starvation or nitrogen starvation for 4 hr. Autophagy activity was assessed by translocation of GFP-Atg8 into vacuoles, as judged by confocal microscopy. n = 300 cells pooled from three independent experiments. Data are presented as means ± SD. ***$p < 0.001$; NS, not significant; two-tailed Student's t tests were used.

(E) Autophagy activity was assessed in cells from (D) by western blot analysis of GFP-Atg8 cleavage. See also Figure S5.

deprivation-induced autophagy may be regulated by a pathway that is distinct from the canonical pathway.

STAR★METHODS

Detailed methods are provided in the online version of this paper and include the following:

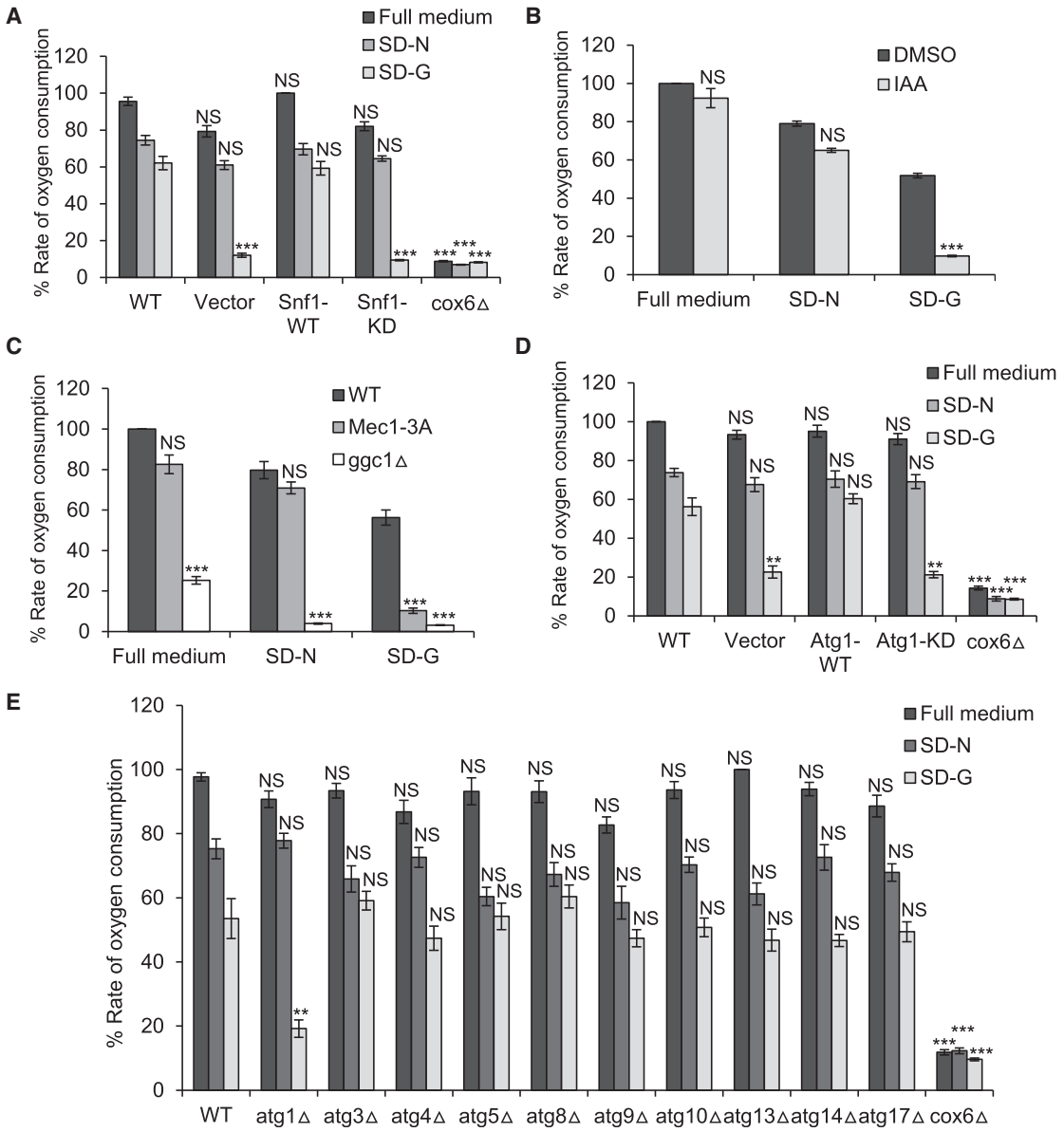

Figure 6. A Snf1-Mec1-Atg1 Module Regulates Mitochondrial Respiration during Glucose Starvation

(A–E) Indicated strains were cultured in SD-G or SD-N for 30 min. Cells were harvested and oxygen consumption was measured using a Clark-type oxygen electrode from a single experiment, n = 3 independent experiments were quantified. Data are presented as means ± SD. ***p < 0.001, **p < 0.001; NS, not significant; two-tailed Student's t tests were used. (A) WT, *snf1*△+empty vector, *snf1*△+ Snf1-WT, *snf1*△+ Snf1-KD, and *cox6*Δ. (B) Mec1-auxin degron strain. (C) WT, Mec1-3A, and ggc1△. (D) WT, *atg1*△+empty vector, *atg1*△+ Atg1-WT, *atg1*△+ Atg1-KD, and *cox6*Δ. (E) WT, *atg1*△, *atg3*△, *atg4*△, *atg5*△, *atg8*△, *atg9*△, *atg10*△, *atg13*△, *atg14*△, *atg17*△, and *cox6*Δ. See also Figures S6–S8.

- ○ Construction of Stable ATR Knockdown Cell Lines and Immunofluorescence Staining
- ○ Auxin Treatment
- ○ Microscopy, Western Blots and Immunoprecipitation
- ○ Purification of FLAG-Tagged Fusion Proteins from Yeast
- ○ Snf1 In Vitro Kinase Assay
- ○ Atg1 In Vitro Kinase Assay
- ○ Determination of Oxygen Consumption
- ○ Mass Spectrometry
- ○ Purification of Yeast Mitochondria
- ○ Identification of the Adaptor Protein Ggc1
- ○ Detection of Snf1 Kinase Activity
- ○ ALP Assay
- ● QUANTIFICATION AND STATISTICAL ANALYSIS

SUPPLEMENTAL INFORMATION

Supplemental Information includes seven figures and two tables and can be found with this article online at http://dx.doi.org/10.1016/j.devcel.2017.03.007.

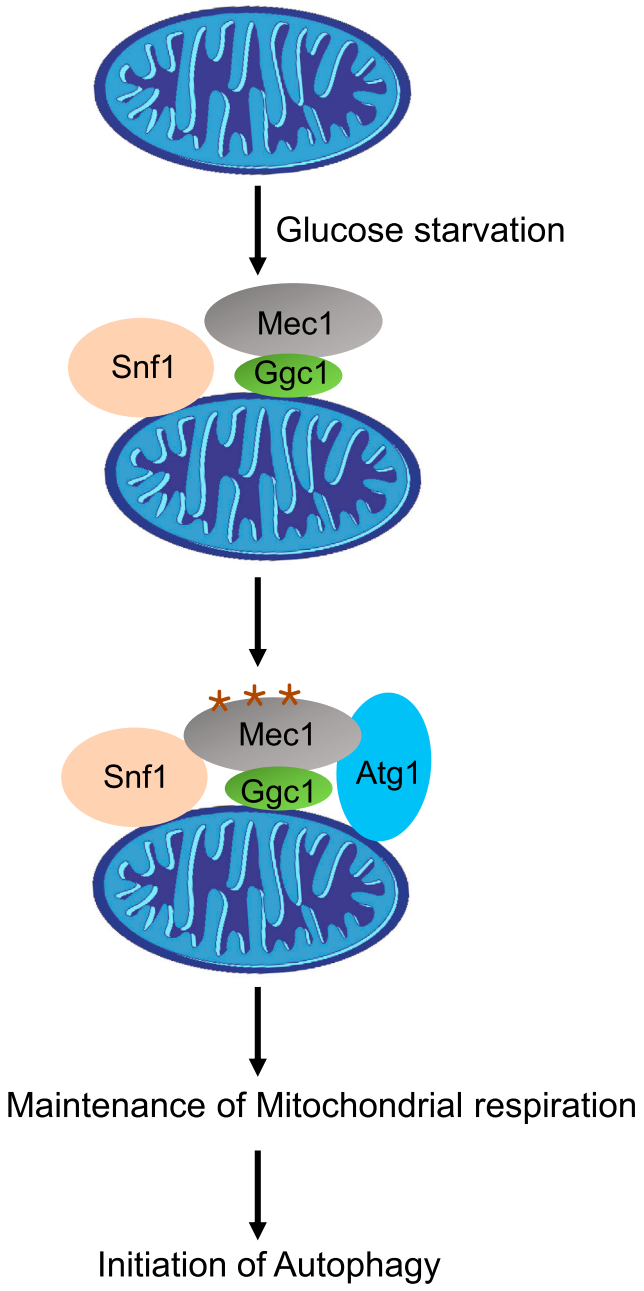

Figure 7. Model Illustrating How the Snf1-Mec1-Atg1 Module Regulates Energy Deprivation-Induced Autophagy

In response to glucose starvation, Snf1 phosphorylates Mec1 on the mitochondrial surface which leads to assembly of the Snf1-Mec1-Atg1 module on mitochondria. The Snf1-Mec1-Atg1 module maintains mitochondrial respiration and promotes the association of Atg1 with Atg13, thereby initiating autophagy. * indicates phosphorylation of Mec1 by Snf1.

AUTHOR CONTRIBUTIONS

C.Y., J.T., H.L., and L.Y. conceived the experiments; L.Y. wrote the paper and supervised the project; C.Y., J.T., P.L., Z.W., J.Z., C.S., N.L., S.X., L.X., L.Y., Y.X., B.J., B.Z., C.D., and Y.H. carried out experiments; L.L., C.S., D.M., and H.D. performed mass spectrometry analysis. All authors discussed the manuscript, commented on the project, and contributed to preparing the paper.

ACKNOWLEDGMENTS

We are grateful to Y. Ohsumi and H. Nakatogawa for antibodies and plasmids. We thank Dr. Bing Zhou for help with oxygen consumption measurements and the yeast gene deletion library, Qiangyou Wan for assistance with protein purification, Ying Li for help with electron microscopy, Jingbo Jiang, Qinghua Zhang, Hui Wang, and Jinlei Yu for purification of mitochondria, and Xingtao Zhou for discussing the manuscript. This research was supported by National Natural Science Foundation of China 31430053, 31321003, Ministry of Science and Technology of the People's Republic of China 2016YFA0500202, Natural Science Foundation of China International Cooperation and Exchange Program 31561143002, Independent Research of Tsinghua University 20161080135, Beijing Natural Science Foundation 5142011, and International Cooperation Grant of Science and Technology 2014DFG32460 to L.Y.

Received: August 11, 2016
Revised: October 31, 2016
Accepted: March 10, 2017
Published: April 10, 2017

REFERENCES

Church, C., Chapon, C., and Poyton, R.O. (1996). Cloning and characterization of PET100, a gene required for the assembly of yeast cytochrome c oxidase. J. Biol. Chem. *271*, 18499–18507.

Emtage, J.L., and Jensen, R.E. (1993). MAS6 encodes an essential inner membrane component of the yeast mitochondrial protein import pathway. J. Cell Biol *122*, 1003–1012.

Ernster, L., and Schatz, G. (1981). Mitochondria: a historical review. J. Cell Biol *91*, 227s–255s.

Graef, M., and Nunnari, J. (2011). Mitochondria regulate autophagy by conserved signalling pathways. EMBO J. *30*, 2101–2114.

Gupta, A., Sharma, S., Reichenbach, P., Marjavaara, L., Nilsson, A.K., Lingner, J., Chabes, A., Rothstein, R., and Chang, M. (2013). .Telomere length homeostasis responds to changes in intracellular dNTP pools. Genetics *193*, 1095–1105.

Gwinn, D.M., Shackelford, D.B., Egan, D.F., Mihaylova, M.M., Mery, A., Vasquez, D.S., Turk, B.E., and Shaw, R.J. (2008). .AMPK phosphorylation of raptor mediates a metabolic checkpoint. Mol. Cell *30*, 214–226.

Hailey, D.W., Rambold, A.S., Satpute-Krishnan, P., Mitra, K., Sougrat, R., Kim, P.K., and Lippincott-Schwartz, J. (2010). .Mitochondria supply membranes for autophagosomes biogenesis during starvation. Cell *141*, 656–667.

Hamasaki, M., Furuta, N., Matsuda, A., Nezu, A., Yamamoto, A., Fujita, N., Oomori, H., Noda, T., Haraguchi, T., Hiraoka, Y., et al. (2013). Autophagosomes form at ER-mitochondria contact sites. Nature *495*, 389–393.

Hines, V., Brandt, A., Griffiths, G., Horstmann, H., Brütsch, H., and Schatz, G. (1990). Protein import into yeast mitochondria is accelerated by the outer membrane protein MAS70. EMBO J. *9*, 3191–3200.

Jackson, S.P. (1996). The recognition of DNA damage. Curr. Opin. Genet. Dev. *6*, 19–25.

Janke, C., Magiera, M.M., Rathfelder, N., Taxis, C., Reber, S., Maekawa, H., Moreno-Borchart, A., Doenges, G., Schwob, E., Schiebel, E., and Knop, M. (2004). A versatile toolbox for PCR-based tagging of yeast genes: new fluorescent proteins, more markers and promoter substitution cassettes. Yeast *21*, 947–962.

Kamada, Y., Yoshino, K., Kondo, C., Kawamata, T., Oshiro, N., Yonezawa, K., and Ohsumi, Y. (2010). Tor directly controls the Atg1 kinase complex to regulate autophagy. Mol. Cell Biol. *30*, 1049–1058.

Karsli-Uzunbas, G., Guo, J.Y., Price, S., Teng, X., Laddha, S.V., Khor, S., Kalaany, N.Y., Jacks, T., Chan, C.S., Rabinowitz, J.D., and White, E. (2014). Autophagy is required for glucose homeostasis and lung tumor maintenance. Cancer Discov. *4*, 914–927.

Kato, R., and Ogawa, H. (1994). An essential gene, ESR1, is required for mitotic cell growth, DNA repair and meiotic recombination in *Saccharomyces cerevisiae*. Nucleic Acids Res. *22*, 3104–3112.

Kim, J., Kundu, M., Viollet, B., and Guan, K.L. (2011). AMPK and mTOR regulate autophagy through direct phosphorylation of Ulk1. Nat. Cell Biol. *13*, 132–141.

Kim, J., Kim, Y.C., Fang, C., Russell, R.C., Kim, J.H., Fan, W., Liu, R., Zhong, Q., and Guan, K.L. (2013). .Differential regulation of distinct Vps34 complexes by AMPK in nutrient stress and autophagy. Cell *152*, 290–303.

Kirisako, T., Baba, M., Ishihara, N., Miyazawa, K., Ohsumi, M., Yoshimori, T., Noda, T., and Ohsumi, Y. (1999). Formation process of autophagosome is traced with Apg8/Aut7p in yeast. J. Cell Biol *147*, 435–446.

Klionsky, D.J. (2010). The molecular machinery of autophagy and its role in physiology and disease. Semin. Cell Dev. Biol. *21*, 663.

Kumar, A., Mazzanti, M., Mistrik, M., Kosar, M., Beznoussenko, G.V., Mironov, A.A., Garrè, M., Parazzoli, D., Shivashankar, G.V., and Scita, G. (2014). ATR mediates a checkpoint at the nuclear envelope in response to mechanical stress. Cell *158*, 633–646.

Li, L., Tan, J., Miao, Y., Lei, P., and Zhang, Q. (2015). ROS and autophagy: interactions and molecular regulatory mechanisms. Cell Mol. Neurobiol. *35*, 615–621.

Majka, J., Niedziela-Majka, A., and Burgers, P.M. (2006). The checkpoint clamp activates Mec1 kinase during initiation of the DNA damage checkpoint. Mol. Cell *24*, 891–901.

Matsuura, A., Tsukada, M., Wada, Y., and Ohsumi, Y. (1997). .Apg1p, a novel protein kinase required for the autophagic process in *Saccharomyces cerevisiae*. Gene *192*, 245–250.

McCartney, R.R., and Schmidt, M.C. (2001). Regulation of Snf1 kinase. Activation requires phosphorylation of threonine 210 by an upstream kinase as well as a distinct step mediated by the Snf4 subunit. J. Biol. Chem. *276*, 36460–36466.

Meisinger, C., Sommer, T., and Pfanner, N. (2000). Purification of *Saccharomcyes cerevisiae* mitochondria devoid of microsomal and cytosolic contaminations. Anal Biochem. *287*, 339–342.

Mitchelhill, K.I., Stapleton, D., Gao, G., House, C., Michell, B., Katsis, F., Witters, L.A., and Kemp, B.E. (1994). .Mammalian AMP-activated protein-kinase shares structural and functional homology with the catalytic domain of yeast Snf1 protein-kinase. J. Biol. Chem. *269*, 2361–2364.

Mizushima, N. (2009). Methods for monitoring autophagy using GFP-LC3 transgenic mice. Methods Enzymol. *452*, 13–23.

Nishimura, K., Fukagawa, T., Takisawa, H., Kakimoto, T., and Kanemaki, M. (2009). .An auxin-based degron system for the rapid depletion of proteins in nonplant cells. Nat. Methods *6*, 917–U978.

Noda, T., and Klionsky, D.J. (2008). The quantitative Pho8Delta60 assay of nonspecific autophagy. Methods Enzymol. *451*, 33–42.

Noda, T., Matsuura, A., Wada, Y., and Ohsumi, Y. (1995). Novel system for monitoring autophagy in the yeast *Saccharomyces cerevisiae*. Biochem. Biophys. Res. Commun. *210*, 126–132.

Ohsumi, Y. (2014). Historical landmarks of autophagy research. Cell Res. *24*, 9–23.

Orlova, M., Barrett, L., and Kuchin, S. (2008). Detection of endogenous Snf1 and its activation state: application to *Saccharomyces* and *Candida* species. Yeast *25*, 745–754.

Paital, B., and Samanta, L. (2013). A comparative study of hepatic mitochondrial oxygen consumption in four vertebrates by using Clark-type electrode. Acta Biol. Hung. *64*, 152–160.

Quintero, M., Colombo, S.L., Godfrey, A., and Moncada, S. (2006). Mitochondria as signaling organelles in the vascular endothelium. Proc. Natl. Acad. Sci. USA *103*, 5379–5384.

Rodriguez, J., and Tsukiyama, T. (2013). ATR-like kinase Mec1 facilitates both chromatin accessibility at DNA replication forks and replication fork progression during replication stress. Genes Dev. *27*, 74–86.

Russell, R.C., Yuan, H.X., and Guan, K.L. (2014). Autophagy regulation by nutrient signaling. Cell Res. *24*, 42–57.

Stephan, J.S., Yeh, Y.Y., Ramachandran, V., Deminoff, S.J., and Herman, P.K. (2010). The Tor and cAMP-dependent protein kinase signaling pathways coordinately control autophagy in *Saccharomyces cerevisiae*. Autophagy *6*, 294–295.

Tanaka, C., Tan, L.J., Mochida, K., Kirisako, H., Koizumi, M., Asai, E., Sakoh-Nakatogawa, M., Ohsumi, Y., and Nakatogawa, H. (2014). Hrr25 triggers selective autophagy-related pathways by phosphorylating receptor proteins. J. Cell Biol *207*, 91–105.

Vozza, A., Blanco, E., Palmieri, L., and Palmieri, F. (2004). Identification of the mitochondrial GTP/GDP transporter in *Saccharomyces cerevisiae*. J. Biol. Chem. *279*, 20850–20857.

Wallace, D.C. (2012). Mitochondria and cancer. Nat. Rev. Cancer *12*, 685–698.

Wang, Z., Jiang, H., Chen, S., Du, F., and Wang, X. (2012). The mitochondrial phosphatase PGAM5 functions at the convergence point of multiple necrotic death pathways. Cell *148*, 228–243.

Weinert, T.A., Kiser, G.L., and Hartwell, L.H. (1994). .Mitotic checkpoint genes in budding yeast and the dependence of mitosis on DNA replication and repair. Genes Dev. *8*, 652–665.

Yamamoto, H., Fujioka, Y., Suzuki, S.W., Noshiro, D., Suzuki, H., Kondo-Kakuta, C., Kimura, Y., Hirano, H., Ando, T., Noda, N.N., et al. (2016). The intrinsically disordered protein Atg13 mediates supramolecular assembly of autophagy initiation complexes. Dev. Cell *38*, 86–99.

Yen, W.L., Legakis, J.E., Nair, U., and Klionsky, D.J. (2007). Atg27 is required for autophagy-dependent cycling of Atg9. Mol. Biol. Cell *18*, 581–593.

Yi, C., Ma, M., Ran, L., Zheng, J., Tong, J., Zhu, J., Ma, C., Sun, Y., Zhang, S., Feng, W., et al. (2012). Function and molecular mechanism of acetylation in autophagy regulation. Science *336*, 474–477.

Zhang, J., Tripathi, D.N., Jing, J., Alexander, A., Kim, J., Powell, R.T., Dere, R., Tait-Mulder, J., Lee, J.H., Paull, T.T., et al. (2015). .ATM functions at the peroxisome to induce pexophagy in response to ROS. Nat. Cell Biol. *17*, 1259–1269.

STAR★METHODS

KEY RESOURCE TABLE

REAGENT or RESOURCE	SOURCE	IDENTIFIER
Antibodies		
Mouse anti-MYC	Roche	11667149001
Mouse anti-GFP	Roche	11814460001
Mouse anti-HA	Abmart	M20003L
Mouse anti-FLAG	Sigma-Aldrich	F1804
Rabbit anti-phospho-AMPKα (Thr172)	Cell Signaling Technology	2535S
Rabbit anti-Phospho-(Ser/Thr) AMPK Substrate	Cell Signaling Technology	5759S
Rabbit anti-PGK1	Nordic Immunology	NE130/7S
Mouse anti-Dpm1	Thermo Fisher Scientific	A6429
Mouse anti-ALP	Thermo Fisher Scientific	A6458
Mouse anti-Pep12	Thermo Fisher Scientific	A21273
Mouse anti-Porin	Thermo Fisher Scientific	A6449
Rabbit anti-Histone H4	Abcam	Ab10158
Rabbit anti-LC3	MBL	PM036
Rabbit anti-ATR	Santa Cruz	SC-1887
Rabbit anti-Actin	Abmart	P30002
Goat anti-Rabbit IgG-HRP	SouthernBiotech	4010-05
Goat anti-Mouse IgG_1-HRP	SouthernBiotech	1070-05
Chemicals, Peptides, and Recombinant Proteins		
Anti-FLAG M2 Affinity Gel	Sigma-Aldrich	A2220
Poly FLAG Peptide lyophilized powder	Biotool	B23111
Rapamycin	Selleck	S1039
Indole-3-acetic acid(IAA)	Sigma-Aldrich	I2886
Protein G Magnetic Beads	Thermo Fisher Scientific	88848
Proteinase K	Sigma-Aldrich	P8811
ssDNA	Sigma-Aldrich	D9156
Zymolyase 20T	mp	08320921
Sorbitol	Sigma-Aldrich	S1876
PNPP	mp	0210087801
MBP	Sigma-Aldrich	M2943
Critical Commercial Assays		
Novex NuPAGE 4-12% Bis-Tris Protein Gels and MOPS SDS Running Buffer	Thermo Fisher Scientific	Cat#NP0342BOX, Cat#NP0323BOX, Cat#NP0001
BCA Protein Assay Kit	Pierce	23227
ClonExpress II One Step Cloning Kit	Vazyme	C112-01
Experimental Models: Cell Lines		
Normal Rat Kidney (NRK) cells	ATCC	CRL-6509
Experimental Models: Organisms/Strains		
S. cerevisiae: Strain background: BY4741	ATCC	201388
S. cerevisiae: BY4741-drived strains; see Table S1	This study	N/A
Recombinant DNA		
GFP-Atg8 in pRS316	Dr. Yoshinori Ohsumi	N/A
GFP-Atg8 in pRS315	This study	N/A
HA-Atg13 in Ycplac111	This study	N/A
HA-Atg13 in Yep352	Dr. Yoshinori Ohsumi	N/A

(*Continued on next page*)

Continued

REAGENT or RESOURCE	SOURCE	IDENTIFIER
Tim23-HA in pRS315	This study	N/A
3XFLAG-Atg1 in pRS316	Dr. Hitoshi Nakatogawa	N/A
3XFLAG-Atg1 KD in pRS316	Dr. Hitoshi Nakatogawa	N/A
HA-Atg1 in pRS316	This study	N/A
HA-Atg1 KD in pRS316	This study	N/A
HA-Snf1 in pRS316	This study	N/A
Sequence-Based Reagents		
Primers for Mec1 Site directed mutagenesis; see Table S2	This study	N/A
Primers for clone Tim23 to pRS316; see Table S2	This study	N/A
Primers for clone Snf1 to pRS316; see Table S2	This study	N/A
Primers for clone Atg13 to Ycplac111; see Table S2	This study	N/A
Primers for clone Atg1 to pRS316; see Table S2	This study	N/A
Software and Algorithms		
ImageJ2	ImageJ	https://imagej.net/Welcome

CONTACT FOR REAGENT AND RESOURCE SHARING

Further information and requests for resources and reagents should be directed to and will be fulfilled by the Lead Contact, Li Yu (liyulab@mail.tsinghua.edu.cn).

EXPERIMENTAL MODEL AND SUBJECT DETAILS

Cell Lines and Cell Culture Conditions

Normal Rat Kidney (NRK) cells from ATCC were cultured in DMEM (Invitrogen) medium supplemented with 10% FBS (Invitrogen) and 50 ug/ml penicillin/ streptomycin. Cells were starved in no-glucose DMEM medium (Invitrogen) supplemented with 10% dialyzed FBS (Invitrogen) and 50 ug/ml penicillin/streptomycin. Transfection of NRK cells was performed through Amaxa nucleofection using solution T and programX-001.

Yeast Strains and Constructs

The wild type BY4741 and deletion derivatives were purchased from Invitrogen. The related strains were generated as described previously (Janke et al., 2004) and verified by PCR analysis of chromosomal DNA and western blot analysis with the corresponding antibody. Expression of all plasmids in yeast was demonstrated by western blotting and sequencing.

METHOD DETAILS

Antibodies

Antibodies were purchased as follows and used at the indicated dilutions: anti-GFP (Roche, 11814460001, 1:2500), anti-MYC (Roche, 11667149001, 1:2500), anti-HA (Abmart, M20003L, 1:2500), anti-FLAG (Sigma, F1804, 1:2500), anti-phospho-AMPKα (Thr172) (Cell Signaling Technology, 2535S, 1:1000), anti-Phospho-(Ser/Thr) AMPK Substrate (Cell Signaling Technology, 5759S, 1: 1000), anti-PGK1 (Nordic Immunology, NE130/7S, 1:10000), anti-Dpm1 (Invitrogen, A6429, 1:2000), anti-ALP (Invitrogen, A6458, 1:2000), anti-Pep12 (Invitrogen, A21273, 1:2000), anti-Porin (Invitrogen, A6449, 1:20000), anti-Histone H4 (Abcam, Ab10158, 1:2500), anti-LC3 (MBL, PM036, 1:1000), anti-ATR (Santa Cruz, SC-1887, 1:250), anti-Actin (Abmart, P30002, 1:5000). Goat Anti-Mouse IgG1, Human ads-HRP (SouthernBiotech, 1070-05, 1:10000) and Goat Anti-Rabbit IgG, Human ads-HRP (SouthernBiotech, 4010-05, 1:10000).

Construction of Stable ATR Knockdown Cell Lines and Immunofluorescence Staining

The pGPU6/hygromycin vector was used for expression of shRNA in NRK cells. The construction of stable ATR knockdown cell lines was performed according to the manufacturer's protocol (Shanghai GenePharma). The efficiency of ATR knockdown was tested by western blotting using anti-ATR antibody. Immunofluorescence staining was performed as described previously (Yi et al., 2012).

Auxin Treatment

Yeast strains were treated with 0.5 mM IAA (indole-3-acetic acid, Sigma, I2886) to induce the degradation of targeted proteins, and the same volume of DMSO was added to control strains (Nishimura et al., 2009; Tanaka et al., 2014).

Microscopy, Western Blots and Immunoprecipitation

Yeast cells with fluorescent tags were cultured to OD_{600}=0.8∼1.0 in selective medium and shifted to SD-G, rapamycin or SD-N medium for different times. The cells were observed using a confocal microscope (FV-1000; Olympus). Extraction of yeast proteins, western blotting and immunoprecipitation were performed as described previously (Yi et al., 2012).

Purification of FLAG-Tagged Fusion Proteins from Yeast

Samples were purified using anti-FLAG M2 resin as follows. For FLAG-tagged Atg1 protein, cells expressing plasmids containing FLAG-tagged Atg1 or Atg1^{D211A} under control of the Cup1 promoter were grown in 4 liters of SD-Ura medium from OD_{600}∼0.2 to OD_{600}∼0.8 at 30°C. $CuSO_4$ was then added to a final concentration of 100 μM to induce expression of Atg1 protein at 30°C for 2 h, after which cells were starved in SD-N medium containing 100 μM $CuSO_4$ at 30°C for 1 h. Whole-cell extracts were obtained by disrupting cells in extraction buffer (350 mM NaCl, 40 mM HEPES [pH 7.5], 10% v/v glycerol, 0.1% Tween-20, 2 μg/ml leupeptin, 2 μg/ml pepstatin A, 5 μg/ml aprotinin, 1 mM phenylmethylsulfonyl fluoride (PMSF), phosphatase inhibitor (Sigma)). For FLAG-tagged Mec1 protein, whole-cell extracts were obtained by collecting *snf1*Δ yeast cells expressing 3XFLAG-Mec1 (Mec1 WT or Mec1^{3A}). Cells were grown to mid-exponential phase (OD_{600}∼ 1.0) in 4 liters of YPD medium or SD-G medium at 30°C. For FLAG-tagged Snf1 protein, *snf1*Δ cells expressing plasmids containing FLAG-tagged Snf1 or Snf1^{kd} under control of the endogenous promoter were grown in 4 liters of SD-Ura medium from OD_{600}∼0.2 to OD_{600}∼1.0 at 30°C. Cells were then starved in SD-G medium at 30°C for 1 h and whole-cell extracts were obtained by disrupting cells in extraction buffer. Samples were centrifuged at 10,000g for 15 min, and the supernatant was transferred to a new tube and further clarified by ultracentrifugation at 40,000g for 1 h. The clarified supernatant was collected and incubated with anti–FLAG M2 resin for 2 h at 4°C. The column was washed 5 times with 20 ml of extraction buffer, and then incubated with 5 bead volumes of extraction buffer including 0.1 mg/ml 3XFLAG peptide (Sigma, F4799) for 1 h at 4°C. Finally, the eluted protein was concentrated to 0.2∼0.5 μg/μl by ultrafiltration with Amicon Ultra centrifugal filters (Millipore) and 25 μl aliquots were stored at -80°C.

Snf1 In Vitro Kinase Assay

3XFLAG-tagged Snf1 WT or Snf1^{kd} protein was purified from the *snf1*Δ yeast strain grown in SD-G medium as above. In vitro kinase assays were performed for 30 min at 30°C in a 40 μl reaction mixture containing ∼200 ng 3X FLAG-Snf1 WT or Snf1^{kd} as kinase, ∼2 μg 3XFLAG Mec1 WT or 3A as substrate, 1 mM ATP in kinase buffer (25 mM HEPES pH7.5, 10 mM $MgCl_2$, 50 mM KCl, 2 mM DTT, 0.1 mM EDTA, 0.1 mM EGTA). The reactions were stopped by boiling in 10 μl 5X SDS sample buffer for 5 min and then resolved by 12% SDS–PAGE and analyzed by immunoblotting using anti-Phospho-(Ser/Thr) AMPK Substrate antibody.

Atg1 In Vitro Kinase Assay

The immunoprecipitated Atg1 proteins were incubated for 60 min at 30°C with kinase buffer (25 mM Hepes, pH7.5, 10 mM $MgCl_2$, 1 mM EGTA, 0.2 mM EDTA, 5 mM NaF, 0.05 mM DTT) and 10 μm cold ATP, 2.5 μCi [gamma- 32P]ATP in a 40 μl reaction with 10 μg of myelin basic protein (MBP) (Sigma, M2941). The reactions were stopped by adding 10 μl 4X protein loading buffer. The samples were separated on SDS-PAGE gels, then analyzed by phosphorimaging with a Typhoon Trio (GE Healthcare).

Determination of Oxygen Consumption

Yeast cells were grown to OD_{600} = 1.0-1.2, and then 30 OD yeast samples were centrifuged, washed and resuspended in SD-G, SD-N or SD medium and incubated for 30 min before measurement. Oxygen consumption was measured using a Clark-type oxygen electrode in a 30 °C constant temperature chamber (Oxygen electrode probe oxel-1, World Precision instruments, Inc. USA) with a total volume of 1 ml of the corresponding medium as the respiration buffer (Paital and Samanta, 2013). The original data were recorded and analyzed using the software ''Chart5 for Windows''. The relative rates of oxygen consumption obtained from different samples are reported as the mean ± SEM.

Mass Spectrometry

For identification of proteins, samples were separated on 4%-12% SDS-PAGE gels. The bands were excised from the gel, reduced with 10 mM DTT, and alkylated with 55 mM iodoacetamide. In-gel digestion was then carried out with sequence-grade modified trypsin (Promega, Fitchburg, WI) in 50 mM ammonium bicarbonate at 37 °C for 2 h. The peptides were extracted twice with 1% trifluoroacetic acid in 50% acetonitrile aqueous solution for 30 min. The extracts were then centrifuged in a SpeedVac to reduce the volume. For LC-MS/MS analysis, the digestion product was separated by a 120 min gradient elution at a flow rate of 0.300 μl/min with an UltiMate 3000 integrated nano-HPLC system, which was directly interfaced with a Thermo Q-Exactive mass spectrometer. The analytical column was a homemade fused silica capillary column (75 μm inner diameter, 150 mm length; Upchurch, Oak Harbor, WA) packed with C-18 resin (300A, 5 μm, Varian, Lexington, MA). Mobile phase A consisted of 0.1% formic acid, and mobile phase B consisted of 100% acetonitrile and 0.1% formic acid. The Q-Exactive mass spectrometer was operated in the data-dependent acquisition mode using Xcalibur 2.2 software and there was a single full-scan mass spectrum in the Orbitrap (400–1800 m/z, 30,000 resolution) followed by 10 data-dependent MS/MS scans in the ion trap at 35% normalized collision energy. The MS/MS spectra from each LC-MS/MS run were searched against the selected database using an in-house Mascot or Proteome Discovery searching algorithm.

Purification of Yeast Mitochondria

Mitochondria were purified according to a previously published method (Meisinger et al., 2000). Yeast were grown to OD_{600}=2∼2.5. The cells were collected or treated with different stressors, washed with Buffer 1 (100 mM Tris-HCl, pH=7.4), and then incubated in Buffer 1 containing 10 mM DTT at 30°C by shaking at 140 rpm for 10 min. Cells were washed with zymolyase buffer (1.2 M sorbitol, 20 mM KPi, pH 7.4), and then incubated at 30°C for 45 min with Zymolyase-20T (5 mg per gram of cells) in zymolyase buffer (7 ml buffer per gram of cells) to obtain protoplasts. The protoplasts were collected by centrifugation at 3,000g for 2 min and washed with Zymolyase buffer. The protoplasts were centrifuged again at 3,000g and 4 °C for 5 min, then resuspended in 6.5 ml ice-cold homogenization buffer (600 mM sorbitol, 10 mM Tris-HCl at pH=7.4, 1 mM EDTA) per microgram of protoplasts and homogenized 12 times using a Dounce homogenizer (50 ml volume). The homogenate was diluted with 1 vol homogenization buffer containing 1 mM PSMF, then centrifuged at 1,500g and 4 °C for 5 min. The supernatant was decanted and centrifuged at 3,000g and 4 °C for 5 min. Mitochondria were pelleted by centrifugation at 12,000g and 4 °C for 15 min. The supernatant was decanted and the pellet was resuspended in SEM (250 mM sucrose, 10 mM MOPS, 1 mM EDTA), and then centrifuged at 12,000g and 4 °C for 15 min. The mitochondria were finally purified by sucrose gradient centrifugation.

Identification of the Adaptor Protein Ggc1

Mitochondria were purified from *snf1*Δ+FLAG-Mec1 and *snf1*Δ (negative control) yeast strains as described above. The mitochondria were disrupted by adding 1% SDS lysis buffer at RT for 1 h, then the lysates were diluted to 0.1% SDS with lysis buffer and FLAG-tagged Mec1 was purified using anti-FLAG M2 resin as described above. The eluted and ultrafiltrated protein was boiled in 5X SDS sample buffer for 5 min and separated on 4%-12% SDS-PAGE gels. After silver staining, the gels were compared and the bands specific to *snf1*Δ FLAG-Mec1 were excised and identified by mass spectrometry (Wang et al., 2012).

Detection of Snf1 Kinase Activity

Yeast were grown to OD_{600}=0.8∼1.2. The cells were collected in full medium or glucose-free medium. Proteins were extracted and samples were separated by SDS-PAGE, The kinase activity of Snf1 was detected by anti-phospho-AMPKα (Thr172) antibody (Orlova et al., 2008)

ALP Assay

Yeast were grown to OD_{600}=0.8∼1.2. The cells were treated with different stimuli. 4 OD_{600} of yeast cells were harvested and washed in 1 ml ice-cold 0.85% NaCl, and resuspended in 200 μl lysis buffer (20 mM PIPES pH 6.8, 50 mM KCl, 100 mM potassium acetate (KOAc), 10 mM $MgSO_4$, 10 μM $ZnSO_4$, 0.5% Triton X-100, 1 mM PMSF). 100 μl acid-washed glass beads were added. The samples were vortexed in the cold room for 5 min, then allowed to rest for 30s. This cycle was repeated 3 times. The samples were added to reaction buffer (250 mM Tris-HCl pH 8.5, 10 mM $MgSO_4$, 10 μM $ZnSO_4$, 0.4 % Triton X-100), then incubated for 30 min at 30°C. Reactions were terminated by adding stop buffer (1 M glycine, pH 11). Samples were monitored by measuring absorbance at 405 nM. Protein concentration was measured using the Pierce BCA assay (Noda and Klionsky, 2008).

QUANTIFICATION AND STATISTICAL ANALYSIS

For all quantitative analyses, mean values are presented together with the standard deviation (s.d., shown as error bars). The number of independent experiments carried out and the related statistics are indicated in each figure legend. Student's two-tailed t-test was used for P-value calculations because all comparisons were between control and experimental conditions. For all other experiments, at least three independent experiments were carried out and a representative result is shown in the respective figures.